

THE EFFECT OF JOINT CLEARANCES ON THE SINGULAR CONFIGURATIONS OF PLANAR PARALLEL MANIPULATORS

MARISE GALLANT AND CLÉMENT GOSSELIN[†]

Département de génie mécanique

Université Laval

Québec, Québec, Canada, G1K 7P4

[†] *corresponding author, gosselin@gmc.ulaval.ca*

Abstract

A two degree-of-freedom (DOF) and a three DOF planar parallel manipulator with prismatic actuated joints are studied in this paper. Joint clearances introduce unconstrained motion to the end-effector of the manipulators. This may cause clearance-free, non-singular configurations to become singular if finite joint clearances are considered. This paper presents a method to find the additional singular configurations that cannot be found by traditional kinematic analysis. Some results for the manipulators studied are also presented.

Résumé

Deux manipulateurs parallèles plans (deux et trois degrés de liberté) avec actionneurs prismatiques sont étudiés dans cet article. Les jeux dans les articulations ainsi que les mouvements à l'organe terminal permis par ceux-ci sont inclus dans l'étude des lieux de singularités. Ainsi, une position de l'organe terminal qui ne correspond pas à une configuration singulière lors d'une étude sans jeu dans les articulations peut le devenir si les jeux ne sont plus nuls. Une méthode pour la détermination des lieux de singularité qui existent en raison de ces jeux est présentée ainsi que des résultats obtenus à l'aide de cette méthode.

1 Introduction

It is a known fact that joint clearances have an important effect on the performance of manipulators. However, this field of research is not very much explored. Joint clearances as well as joint and

link flexibility are determining factors in some areas of research such as positioning accuracy, and kinematic and dynamic performances. (Parenti-Castelli and Venanzi (2002))

This paper will focus on joint clearances only and their effect on the definition or determination of singular configurations. The first part of this paper will present the manipulators studied, their inverse kinematic equations and the determination of their singularity loci with conventional methods.

Many papers exist on the subject of singular configurations and many different ways to deal with this subject may be found (Zlatanov, Fenton, and Benhabib (1998), Sen and Mruthyunjaya (1998), Sefrioui and Gosselin (1994), Bhattacharya et. al.(1998)). The approach used by Gosselin and Angeles (1990) is very well suited for the goals of this paper. Their method divides singularities into three types by using the Jacobian matrices. A manipulator is in a singular configuration when at least one of these matrices has a null determinant. The singularities of type I defined in this paper corresponds to the workspace boundary, type II may be inside of the workspace, and type III is architectural and may be easily avoided at the design stage. Type II singularities are also known as platform or parallel singularities. Sefrioui and Gosselin (1992, 1995) developed a software with which analytical expressions for the singularity loci were obtained and superimposed on a manipulator's workspace. These analytical expressions were obtained by computing the determinants of the Jacobian matrices and equating them to zero.

The adopted joint clearance model will then be presented, as well as the manner in which joint clearances introduce possible unconstrained motion to the end-effector (EE) of the two planar parallel manipulators under study in this paper. Some authors choose to model joint clearances by adding extra links, either actuated or not (Ting et. al.(2000), Grant and Fawcett (1979)). Others, such as Wang and Roth (1989), have studied position errors by identifying all possible contact modes in a revolute joint ; position errors are computed according to the external forces applied. Voglewede and Ebert-Uphoff (2002) have studied the unconstrained motion caused by joint clearances and the effect of different types of neighboring singularities on the extent of this unconstrained motion ; for locked actuators, the possible unconstrained motion due to joint clearances are computed in the same way as workspaces would be. This same approach is used in this paper. The method chosen to determine the workspace is the one found in Gosselin (1990) because it may very easily be implemented in computer programming. Boundaries of a workspace are simply composed of

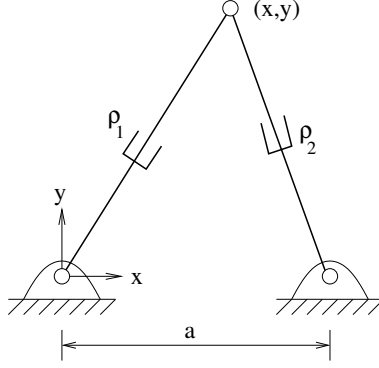


Figure 1: Two DOF planar parallel manipulator with prismatic actuators.

sphere portions (in $3D$) or arcs portions (in $2D$) for a constant orientation of the EE.

The approach based on the unconstrained motion will show how joint clearances introduce singular configurations that would not be singular in the clearance-free kinematic study of a manipulator. The procedure used to find these additional singular configurations will also be described as well as the obtained results.

2 Two DOF and three DOF Planar Parallel Manipulators and Their Inverse Kinematic Equations

The two DOF planar parallel manipulator studied in this paper is shown in Figure 1. Two revolute passive joints are attached to a fixed base on the x axis at $x = 0$ and $x = a$. The two actuated prismatic joints ρ_1 and ρ_2 are attached at one end to the revolute joints on the base. At the other end, they are attached at the same point to passive revolute joints where is located the EE that can be positioned in the xy plane.

The inverse kinematic equations for this manipulator are :

$$\rho_1^2 = x^2 + y^2 \quad \text{and} \quad \rho_2^2 = (x - a)^2 + y^2 \quad (1)$$

The three DOF planar parallel manipulator also to be studied is shown in Figure 2. It is composed of a triangular fixed base where vectors \mathbf{r}_1 , \mathbf{r}_2 and \mathbf{r}_3 prescribe its shape and size. A triangular mobile platform is prescribed by vectors \mathbf{s}_{10} , \mathbf{s}_{20} and \mathbf{s}_{30} in the platform's local coordinate system $(O'x'y')$, which are vectors $\mathbf{s}_1, \mathbf{s}_2$ and \mathbf{s}_3 in Oxy (shown in the figure). The EE is located at

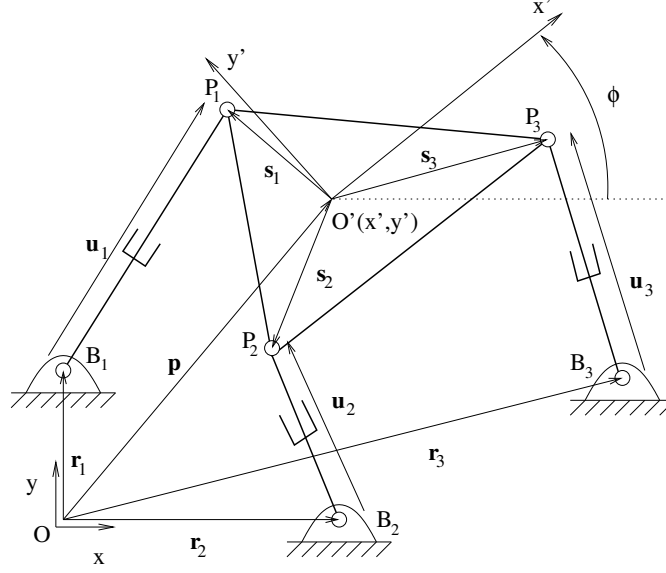


Figure 2: Three DOF planar parallel manipulator with prismatic actuators.

the origin of the platform's local coordinate system. The base and the platform are joined by three RPR (revolute-prismatic-revolute) kinematic chains where the three prismatic joints ρ_1, ρ_2, ρ_3 are actuated. Their lengths are given by :

$$\rho_i^2 = \mathbf{u}_i^T \mathbf{u}_i, \quad i = 1, 2, 3 \quad (2)$$

The output of the manipulator is the position $\mathbf{p} = [x, y]^T$ of the EE and its orientation ϕ . The orientation matrix is thus :

$$\mathbf{Q} = \begin{bmatrix} \cos \phi & -\sin \phi \\ \sin \phi & \cos \phi \end{bmatrix} \quad (3)$$

For each leg of the manipulator, the following equation can be written :

$$\mathbf{u}_i = \mathbf{p} + \mathbf{s}_i - \mathbf{r}_i, \quad i = 1, 2, 3 \quad (4)$$

To obtain the inverse kinematic equations, the above equations (4) are substituted into equations 2:

$$\rho_i^2 = (\mathbf{p} + \mathbf{Q}\mathbf{s}_{i0} - \mathbf{r}_i)^T (\mathbf{p} + \mathbf{Q}\mathbf{s}_{i0} - \mathbf{r}_i), \quad i = 1, 2, 3 \quad (5)$$

with :

$$\mathbf{s}_i = \mathbf{Q}\mathbf{s}_{i0}, \quad i = 1, 2, 3 \quad (6)$$

3 Singular Configurations

The Jacobian matrices are obtained by differentiating the inverse kinematic equations obtained in the previous section with respect to time in order to obtain the following form :

$$\mathbf{A}\dot{\mathbf{x}} + \mathbf{B}\dot{\boldsymbol{\rho}} = \mathbf{0} \quad (7)$$

where $\dot{\mathbf{x}}$ is the velocity of the end-effector $[\dot{x}, \dot{y}]^T$ for the two DOF manipulator and $[\dot{x}, \dot{y}, \dot{\phi}]^T$ for the three DOF manipulator, $\dot{\boldsymbol{\rho}}$ is the vector containing the actuator velocities $[\dot{\rho}_1, \dot{\rho}_2]^T$ (two DOF) and $[\dot{\rho}_1, \dot{\rho}_2, \dot{\rho}_3]^T$ (three DOF), and where \mathbf{A} and \mathbf{B} are the Jacobian matrices of the manipulators.

In the case of the two DOF manipulator, these matrices are easily found :

$$\mathbf{A} = \begin{bmatrix} -x & -y \\ a-x & -y \end{bmatrix} \quad \text{and} \quad \mathbf{B} = \begin{bmatrix} \rho_1 & 0 \\ 0 & \rho_2 \end{bmatrix} \quad (8)$$

The singular configurations of the manipulator are obtained by computing the determinant of the matrices and equating them to zero. Matrix \mathbf{B} is singular when one of the actuators has a length of zero. The physical interpretation is that at least one of the actuators is at one of its physical limits : its minimal or maximal length. These singularities are located on the boundaries of the workspace.

The two DOF matrix \mathbf{A} is singular when $y = 0$, which corresponds to the two prismatic actuators being aligned on the x axis. The EE instantaneously gains a degree of freedom even with its actuators locked ; it cannot apply or withstand a force in the y direction.

The two types of singularities presented above are often referred to as type I and type II singularities (Gosselin, 1990).

If we repeat the preceding procedure for the three DOF manipulator, we obtain :

$$2\rho_i\dot{\rho}_i = 2(\mathbf{p} + \mathbf{s}_i - \mathbf{r}_i)^T(\dot{\mathbf{p}} + \dot{\phi}\mathbf{E}\mathbf{Q}\mathbf{s}_{i0}), \quad i = 1, 2, 3 \quad (9)$$

where

$$\dot{\mathbf{Q}} = \dot{\phi} \mathbf{E} \mathbf{Q} \quad (10)$$

and

$$\mathbf{E} = \begin{bmatrix} 0 & -1 \\ 1 & 0 \end{bmatrix} \quad (11)$$

Equation (9) may be written :

$$\rho_i \dot{\rho}_i = (\mathbf{p} + \mathbf{s}_i - \mathbf{r}_i)^T \dot{\mathbf{p}} + (\mathbf{p} + \mathbf{s}_i - \mathbf{r}_i)^T \dot{\phi} \mathbf{E} \mathbf{Q} \mathbf{s}_{i0}, \quad i = 1, 2, 3 \quad (12)$$

or

$$\rho_i \dot{\rho}_i = \mathbf{u}_i^T \dot{\mathbf{p}} + \dot{\phi} \mathbf{u}_i^T \mathbf{E} \mathbf{Q} \mathbf{s}_{i0}, \quad i = 1, 2, 3 \quad (13)$$

Matrix \mathbf{B} is simply a 3×3 diagonal matrix with elements ρ_1 , ρ_2 and ρ_3 . If the above equations are presented in the same form as equation (7), the following \mathbf{A} and \mathbf{B} matrices are obtained :

$$\mathbf{A} = \begin{bmatrix} \mathbf{u}_1^T \mathbf{E} \mathbf{Q} \mathbf{s}_{10} & \mathbf{u}_1^T \\ \mathbf{u}_2^T \mathbf{E} \mathbf{Q} \mathbf{s}_{20} & \mathbf{u}_2^T \\ \mathbf{u}_3^T \mathbf{E} \mathbf{Q} \mathbf{s}_{30} & \mathbf{u}_3^T \end{bmatrix} \quad \text{and} \quad \mathbf{B} = \begin{bmatrix} \rho_1 & 0 & 0 \\ 0 & \rho_2 & 0 \\ 0 & 0 & \rho_3 \end{bmatrix} \quad (14)$$

A type II singularity will occur if vectors $\mathbf{u}_1, \mathbf{u}_2$ and \mathbf{u}_3 intersect at a single point or at infinity (when they are parallel). An analytical expression for the singularity loci is obtained by equating the determinant of matrix \mathbf{A} to zero. This expression is a quadratic equation in the xy plane for a constant orientation of the EE : $0 = A_1 x^2 + A_2 xy + A_3 x + A_4 y^2 + A_5 y$, where the coefficients (A_i , $i = 1, 2, 3, 4, 5$) are a function of the architectural parameters of the manipulator and the orientation of the EE.

4 Joint Clearance Model and Unconstrained EE Motion

A simple one DOF clearance model is adopted in this paper. The effect of the clearance of the passive revolute joints on the extremities of each leg are considered. Figure 3 shows a much exaggerated clearance in a revolute joint. Its value is defined as the distance between the center of the hole and that of the pin when there is contact between the two parts.

When the actuators (prismatic joints) are locked, an unconstrained motion of the EE is possible due to the joint clearances. Depending on the forces and moments applied to the EE, compression

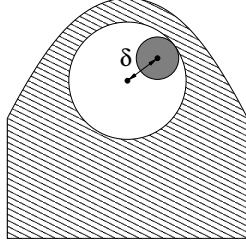


Figure 3: Clearance model.

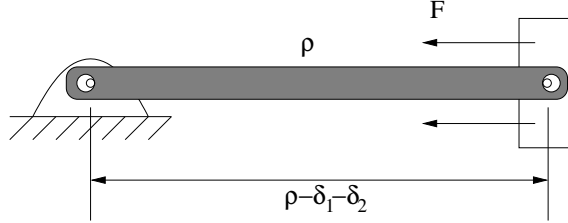


Figure 4: Effect of clearance on leg length.

or tensile forces will be transmitted to the legs. In the first case, the length of the leg will be $\rho - \delta_1 - \delta_2$, and in the latter $\rho + \delta_1 + \delta_2$. Figure 2 shows this clearly. ρ is the length of the leg measured between the center of each hole. If the forces are of compression, the leg will be shortened by the amount of both clearances : $-(\delta_1 + \delta_2)$. In the event of traction forces, the legs will gain $\delta_1 + \delta_2$. The two joint clearances are always taken into account together, therefore, they will be replaced by δ in the remainder of this article ($\delta = \delta_1 + \delta_2$). It will also be assumed that the same clearances are present in all legs.

For both manipulators studied, the unconstrained motion is defined in the same manner as the workspace would be defined except for the minimum and maximum lengths of the actuators used in their computation.

For the two DOF manipulator, the unconstrained motion is the intersection of two thin rings centered at $x = 0$ and $x = a$ with radii of $\rho_i - \delta$ and $\rho_i + \delta$, $i = 1, 2$.

The unconstrained motion of the three DOF manipulator is more complex, because it is tridimensional (x, y, ϕ) . The approach used in this paper consists of computing, for locked actuators, first the constant orientation workspace for the prescribed orientation ϕ , then varying ϕ by a chosen increment $\Delta\phi$, and computing the constant orientation workspace until such a workspace ceases to exist. The final 3D workspace is discretized along ϕ where each slice ($\phi = \text{constant value}$) is the

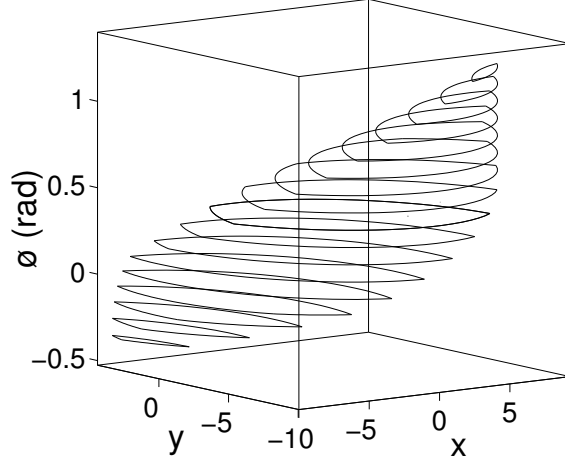


Figure 5: 3D workspace discretized along ϕ .

exact xy workspace. An example is shown in Figure 5.

The inverse kinematic equations (5) can be expanded and the terms collected to obtain the following form :

$$\rho_i^2 = (x - a_i)^2 + (y - b_i)^2 \quad i = 1, 2, 3 \quad (15)$$

where :

$$\begin{aligned} a_i &= r_{ix} - s_{i0x} \cos \phi + s_{i0y} \sin \phi \\ b_i &= r_{iy} - s_{i0x} \sin \phi - s_{i0y} \cos \phi \quad i = 1, 2, 3 \end{aligned} \quad (16)$$

Terms a_i and b_i for $i = 1, 2, 3$ are expressed in the fixed coordinate system located at the base of the manipulator. The r and s terms are architectural parameters and were defined previously, when the three DOF manipulator was first presented. If the orientation, ϕ , is constant, a_i and b_i for $i = 1, 2, 3$ become constant. If they are constant, equations (15) are those of circles. The constant orientation workspace corresponds to the intersection of the three annular regions obtained from equations (15) and the minimum and maximum values of the leg lengths :

$$\rho_i - \delta, \quad \rho_i + \delta, \quad i = 1, 2, 3 \quad (17)$$

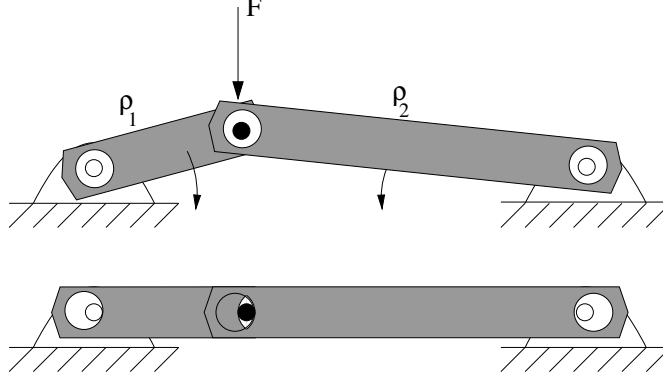


Figure 6: Two DOF manipulator in singularity configuration because of joint clearances.

5 Effect of Joint Clearances on the Singularity Loci

It is simple to show with the two DOF manipulator the effect of finite clearances on the singular configurations. It is known that the EE cannot withstand a force in the y direction when both legs are aligned on the x axis. If clearances are taken into account, and if the EE is close enough to the x axis, the unconstrained motion may allow the EE to be in a singular configuration. This situation can be observed in Figure (6). In this figure, the force F applied to the EE is directed towards the x axis. This force will take the EE to the other side of the x axis (the other possible solution to the direct kinematic equations), since the manipulator cannot resist this force.

With this two DOF manipulator, it is possible to find an analytical expression that represents the envelope of all configurations that may become singular due to finite joint clearances. With no joint clearance, another way to express singular configurations for the two DOF manipulator other than $y = 0$ is :

$$\begin{aligned}
 \rho_1 + \rho_2 = a & \quad \text{if } 0 \leq x \leq a \\
 \rho_1 - \rho_2 = a & \quad \text{if } x > a \\
 \rho_2 - \rho_1 = a & \quad \text{if } x < a
 \end{aligned} \tag{18}$$

This last definition is very helpful for the determination of the singularity area when joint clearances are considered. Equations (18) becomes :

$$\begin{aligned}
(\rho_1 - \delta) + (\rho_2 - \delta) &= a & \text{if } 0 \leq x \leq a \\
(\rho_1 + \delta) - (\rho_2 - \delta) &= a & \text{if } x > a \\
(\rho_2 + \delta) - (\rho_1 - \delta) &= a & \text{if } x < a
\end{aligned} \tag{19}$$

By substituting the inverse kinematic equations (1) in equation (19) and isolating y , we obtain the analytical expressions sought.

It is impossible to follow the same steps with the three DOF manipulator. It is also impossible to find an analytical expression which represents the limits of the area enveloping the singularity curves that also constitutes singular configurations. Discretization is needed.

In order to better visualize and understand what happens with the three DOF manipulator, one prescribed orientation (ϕ_p) at a time will be studied. However, the unconstrained motion considered will take varying orientations into account, since an unconstrained rotation will exist.

The procedure used is outlined in Figure 7. Starting with ϕ_p , determine the singularity loci curves, discretize to make a list of points : $(x_i, y_i) \ i = 1...n$. For each xy pair, determine corresponding leg lengths. Taking joint clearances into account, determine and plot the ϕ_p constant orientation workspace of the unconstrained motion (for each xy pair).

The steps described above are then repeated in a loop, but with some important modifications. ϕ is incremented and the new singularity loci curves are computed and then discretized into a list of points. The unconstrained motion workspace is computed in $3D (xy\phi)$ for each xy pair obtained from new ϕ . An example of a $3D$ workspace discretized along ϕ was shown earlier in Figure 5.

If ϕ_p is included in the $3D$ workspace, this $2D$ slice of the $3D$ workspace is plotted along with the others obtained in the first part of the procedure. ϕ is incremented and the loop is repeated if at least one slice was plotted during the last loop, $i = 1...n$. Once the procedure is completed, the result is a cloud of relatively small workspaces representing the areas where the 3 DOF manipulator may be in a singular configuration.

6 Results

In the results presented, the distance a between the revolute joints at the base of the two DOF manipulator is set to 1. The minimum and maximum leg lengths are set to 0.2 and 1.5, respectively.

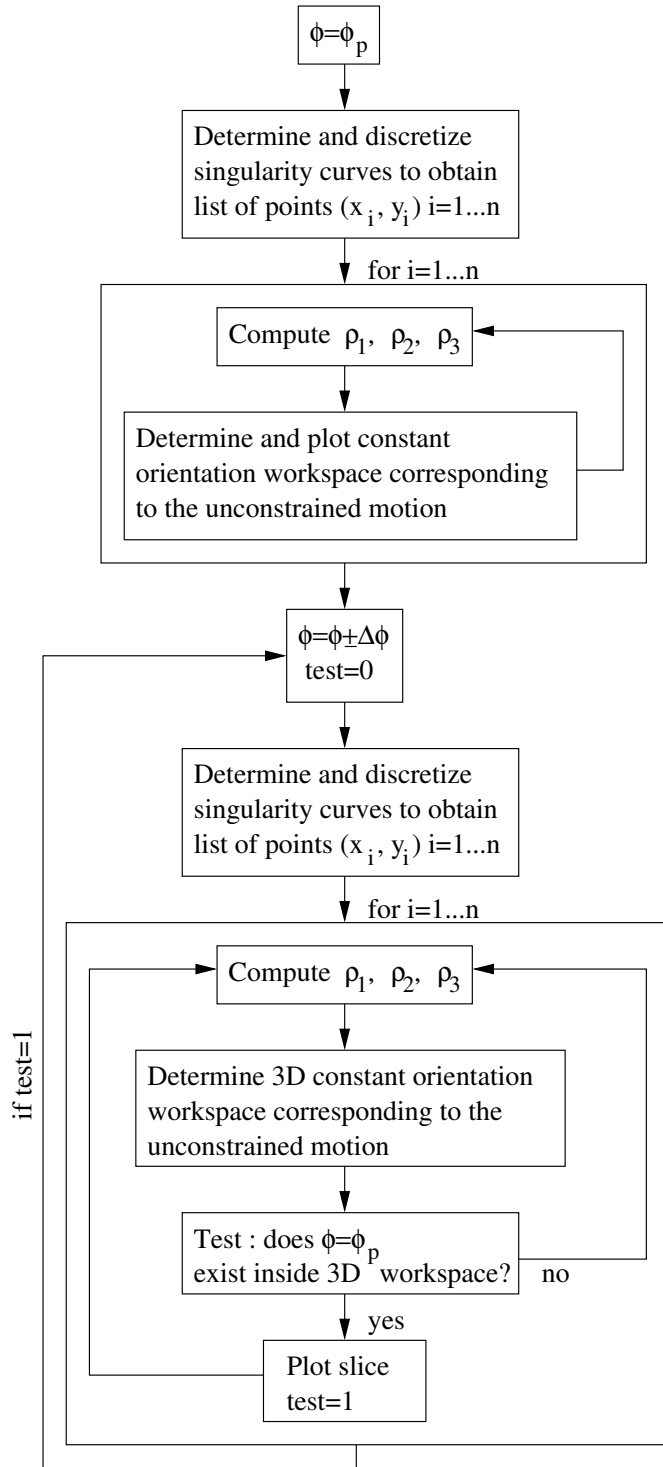


Figure 7: Algorithm for the determination of all singular configurations of the 3 DOF manipulator.

In Figure 8, the workspace for the chosen range of ρ_1 and ρ_2 is plotted. The arcs with the smaller radii (0.2) correspond to the minimum leg length and are holes inside of the workspace. In order to avoid singular configurations, the EE of the manipulator must stay out of the delimited area shown. The figure shows how this area varies according to the clearance value ($0 \leq \delta \leq 0.020$).

The architecture of the three DOF manipulator is summarized in Table 1. The clearance value, δ , is set at $\delta = 0.05$ for all results presented. In Figures 9 and 10, the singular configurations correspond to the areas in black. The clearance-free singularity curves are traced on these areas in white. The prescribed orientations are $\phi = 60^\circ$ and $\phi = 65^\circ$, respectively. The constant orientation workspace can also be seen.

Some prescribed orientations may bring unwanted surprises. The quadratic nature of the singularity loci permits the curves to be elliptic, hyperbolic or parabolic depending on the orientation (and architecture) of the manipulator (Sefrioui and Gosselin (1995)). If the prescribed orientation is close enough to a transition between elliptic, parabolic, and hyperbolic curves, areas of the manipulator's workspace that would seem a safe distance away from the singularity loci might not be as far from singularities as originally thought. In these transition areas, the singularity loci change more rapidly along ϕ . A situation like this exists for $\phi = 50^\circ$, as shown in Figure 11. The transition happens close to $\phi = 54.4^\circ$.

In order to see how the unconstrained motion workspace may cause a configuration to be singular, Figure 12 has been added. One point from Figure 9 that is clearly located in the singular area $(x, y) = (-10, 5)$ was chosen. The leg lengths were computed, then the unconstrained motion workspace was computed and plotted in 3D as well as the singularity surface in that area. It is possible to see in this figure that both intersect in two places. Because the motion in the plotted workspace is unconstrained, it is possible for the manipulator to be in a singular configuration.

7 Conclusion

The effect of joint clearances on the singularity loci of two planar parallel RPR manipulators with two DOF and three DOF was studied. It was found that their effect was non-negligible. In some cases, the extent of their effect may even be surprising, especially when the prescribed orientation is close to where the changes in the singularity loci are abrupt.

Base	Platform
$\mathbf{r}_1 = (0, 0)$	$\mathbf{s}_{10} = (0, 0)$
$\mathbf{r}_2 = (16, 0)$	$\mathbf{s}_{20} = (17, 0)$
$\mathbf{r}_2 = (0, 10)$	$\mathbf{s}_{20} = (13, 16)$
$5 \leq \rho_i \leq 25, i = 1, 2, 3$	

Table 1: Architectural Parameters of the three DOF Manipulator.

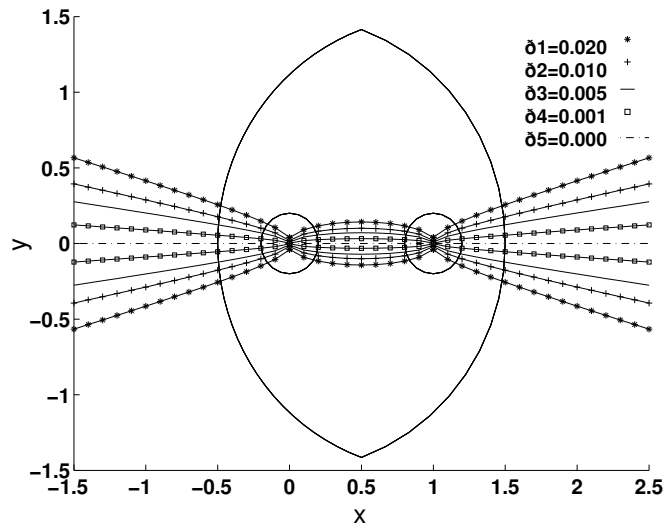


Figure 8: Singular areas as a function of the clearance value.

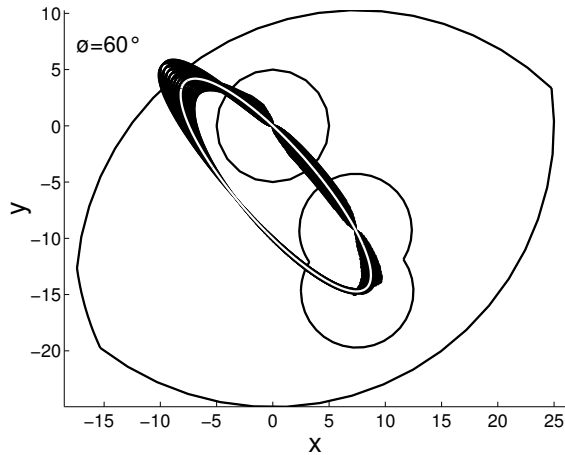


Figure 9: Singular areas of three DOF manipulator at orientation of 60 degrees.

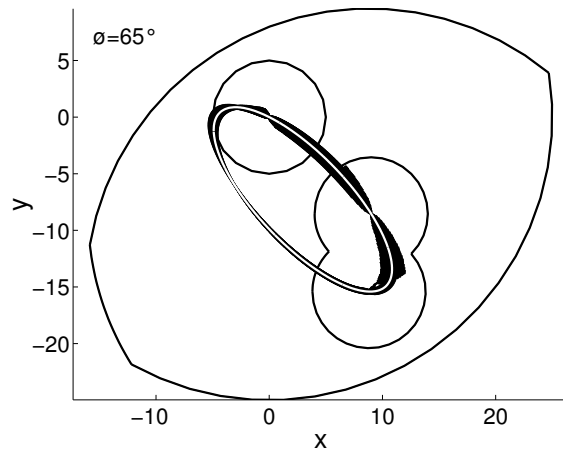


Figure 10: Singular areas of three DOF manipulator at orientation of 65 degrees.

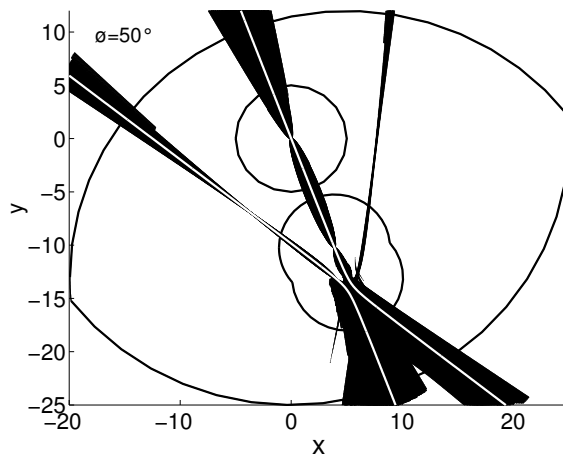


Figure 11: Singular areas of three DOF manipulator at orientation of 50 degrees.

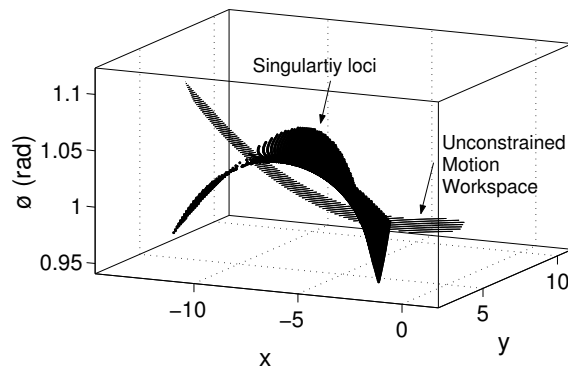


Figure 12: Unconstrained motion workspace at one prescribed point, and singularity loci.

Since the determination of the areas of singular configurations for a prescribed orientation is non-intuitive, it is important to consider how the tolerances and joint clearances may change the kinematic properties of the manipulator at its design stage.

8 Acknowledgment

This research was funded by a NSERC grant.

References

- [1] Parenti-Castelli, V., Venanzi, S. (2002). On the Joint Clearance Effects in Serial and Parallel Manipulators. Proceedings of the Workshop on Fundamental Issues and Future Research Directions for Parallel Mechanisms and Manipulators. Quebec City.
- [2] Zlatanov, D., Fenton, R. G., Benhabib, B. (1998). Identification and classification of the singular configurations of mechanisms. *Mechanism and Machine Theory*, 33 (6), 743-760.
- [3] Sen, D., Mruthyunjaya, T. S. (1998). A centro-based characterization of singularities in the workspace of planar closed-loop manipulators. *Mechanism and Machine Theory*, 33 (8), 1091-1104.
- [4] Sefrioui, J., Gosselin, C. M. (1994). Étude et représentation des lieux de singularité des manipulateurs parallèles sphériques à trois degrés de liberté avec actionneurs prismatiques. *Mechanism and Machine Theory*, 29 (4), 559-579.
- [5] Bhattacharya, S., Hatwal, H., Ghosh, A. (1998). Comparison of an exact and an approximate method of singularity avoidance in platform type parallel manipulators. *Mechanism and Machine Theory*, 33 (7), 965-974.
- [6] Gosselin, C., Angeles, J. (1990). Singularity analysis of closed-loop kinematic chains. *IEEE Transactions on Robotics and Automation*, 6 (3), 281-290.
- [7] Sefrioui, J., Gosselin, C. M. (1992). Singularity analysis and representation of planar parallel manipulators. *Robotics and Autonomous Systems*, 10, 209-224.

- [8] Sefrioui, J., Gosselin, C. M. (1995). On the quadratic nature of the singularity curves of planar three-degree-of-freedom parallel manipulators. *Mechanism and Machine Theory*, 30 (4), 533-551.
- [9] Ting, K.-L., Zhu, J., Watkins, D. (2000). The effects of joint clearance on position and orientation deviation of linkages and manipulators. *Mechanism and Machine Theory*, 35, 391-401.
- [10] Grant, S. J., Fawcett, J. N. (1979). Effects of clearance at the coupler-rocker bearing of a 4-bar linkage. *Mechanism and Machine Theory*, 14, 99-110.
- [11] Wang, H. H. S. et Roth, B. (1989). Position errors due to clearances in journal bearings. *Journal of Mechanisms, Transmissions, and Automation in Design*. 111, 315-320.
- [12] Voglewede, P. A., Ebert-Uphoff, I. (2002). Two viewpoints on the unconstrained motion of parallel manipulators at or near singular configurations. *Proceedings of the Workshop on Fundamental Issues and Future Research Directions for Parallel Mechanisms and Manipulators*. Quebec City.
- [13] Gosselin, C. (1990). Determination of the workspace of 6-dof parallel manipulators. *Journal of Mechanical Design*, 112, 331-336.